RSC Advances

ROYAL SOCIETY OF CHEMISTRY

www.rsc.org/advances

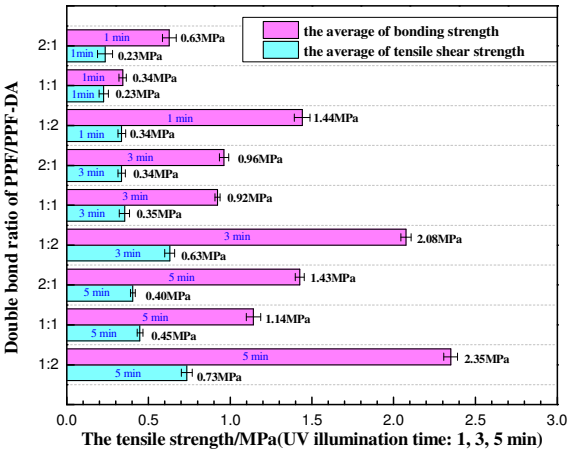

The cured PPF/PPF-DA polymer networks material can be used as a LEDs encapsulant, owing to suitable refractive index, high transparency, appropriate tensile strength, and excellent thermal stability.

Light emitting diodes (LEDs) encapsulation of polymer composites based on poly(propylene fumarate) crosslinked with poly(propylene fumarate)-diacrylate

Liang Wang, Da-Gang Guo,* Hui Zhu and Lei Xie

State Key Laboratory for Mechanical Behavior of Materials, School of Materials Science and Engineering, Xi'an Jiaotong University, Xi'an 710049, China
e-mail: guodagang@mail.xjtu.edu.cn

A novel poly(propylene fumarate)-based polymer networks with good performance for high-power light emitting diodes (LEDs) encapsulation was introduced in this research. Polymer networks have been prepared by radical polymerization using poly(propylene fumarate) (PPF) and poly(propylene fumarate)-diacrylate (PPF-DA) macromers with photo-initiator systems. Photo-crosslinking was accomplished with BAPO accelerated by UV irradiation. It provided an effective curing behavior. PPF and PPF-DA were characterized by Fourier-transform infrared spectroscopy and ^{1}H NMR. The thermal gravity analysis showed that the PPF/PPF-DA (double bond ratios 0.5, 1, and 2) encapsulation material were stable below 287.98 ^{o}C, 285.26 ^{o}C and 271.60 ^{o}C, respectively. The mechanical properties experiments indicated that bonding strength was in the range of 1.09±0.04 MPa to 2.39±0.04 MPa and tensile-shear strength ranged from 0.38±0.02 MPa to 0.79±0.03 MPa. The cured PPF/PPF-DA networks can be used as a LEDs encapsulant, owing to suitable refractive index (n=1.537-1.541), high transparency (98.75%), appropriate tensile strength, and excellent thermal stability.

1. Introduction

Energy-savings are getting more and more important in recent years, since both global warming and energy reduction turns gradually serious. Light emitting diodes (LEDs) (**Fig. 1**) is a very essential application for energy-savings nowadays.[1] LEDs possess many favorable characteristics, such as higher luminosity at low currents and voltages, longer service life, versatility in a variety of colors, environmental friendliness, higher resistance to vibration, and higher tolerance to repeated power switching.[2-4] Currently, LEDs have been widely applied in many fields, including displaying, ordinary illumination, communications, medical services and demonstration [2-4].

Fig. 1 Photograph of the Light emitting diode (LED).

Recently, Looking for a new selective LED encapsulant is a fascinating topic. Particularly, the newly-generation LED products with the characteristics of cheap, energy saving and easily accessible has been proposed and thus further opened new fields for polymer synthesis.[5] Therefore, it is essential to design a LED encapsulant which is reliable with excellent thermal stability and has great energy efficiency with a high refractive index. Currently, the major materials that have been used as LED encapsulations are epoxy resins and silicone resins.[6-7] Epoxy resins are versatile and have been the standard choice for encapsulation of indicator LEDs because of their low cost, low dielectric constant, good adhesive properties, etc.[8-9]

As is well known, PPF-based polymer is one of much attractive polymers, which has been under investigation as a biodegradable and crosslinkable polymer composite for use in orthopedic applications for many years.[10-12] However, there is almost no literature reports about its application in the encapsulation adhesive. Poly(propylene fumarate) (PPF) is an unsaturated linear polyester with fumarate double bonds that can be cross-linked *in situ*.[13-14] The unsaturated carbon-carbon bonds of the fumaric acid unit that allow cross-linking of the polymer into a covalent polymer network.[15] The principle disadvantage of PPF is that it is a viscous liquid at room temperature,

making handling of the polymer somewhat cumbersome.[16] Similarly, PPF-diacrylate is based upon the same repeat unit as PPF, containing ester groups. PPF-DA has been explored in combination with PPF for the formation of cross-linked, polymer networks with tunable material properties. The networks have demonstrated high strength and low water absorption.[17] The initiator system, which controls the crosslinking reaction, can also influence the properties of the networks.[15] The strongest networks were formed with a bis(2,4,6-trimethylbenzoyl) phenophosphine oxide (BAPO) photo-initiator activated by ultraviolet light. In the frame of our works on the design of LED encapsulant, we propose here to develop BAPO as photoinitiators of PPF and PPF-DA upon highly attractive near UV or visible LED lights. The mechanical properties can be controlled by varying the crosslinking density through the ratio of PPF and PPF-DA components in the network, and which dependent upon the molecular characteristics of the constituent polymer.[18-20] The cross-linked reaction behavior indicates that the acrylate bond participated more in the formation of the PPF/PPF-DA polymer networks. This increase is attributed to the greater reactivity of the acrylates as well as the biased affinity of both groups toward the acrylate bond. The behavior has been observed with similar fumarate-acrylate radical copolymerizations.[21] Accordingly, PPF-based polymer networks can be fabricated with a wide range of controllable properties as needed for specific applications through manipulation of tunable polymer parameters.

In the present paper, we attempt to synthesize a PPF-based polymer networks using PPF-diacrylate (PPF-DA) as a crosslinking reagent to develop a novel LED encapsulant. We investigated the effects of double bond ratio of PPF/PPF-DA on the optical properties and mechanical properties of the cross-linked polymer networks. In addition, PPF/PPF-DA composite materials thermal behaviors are also studied by differential scanning calorimeter (DSC) and thermal gravimetric analysis (TGA). The thermal analysis exhibits either mass loss or gain due to decomposition, oxidation, or loss of volatiles. Most notably, an enhanced thermal resistance at 280 ^{o}C was achieved for this polymer, which has not been reported to our knowledge for any other commercial LED encapsulant having such a high refractive index of up to 1.541. The novel poly(propylene fumarate)-based polymer networks encapsulant can provide stable optical clarity for high operating temperatures and high brightnesses of LEDs.

2. Experimental section

2.1. Materials

The raw chemical reagents, including fumaryl chloride, diethyl fumarate, hydroquinone, anhydrous potassium carbonate, Bis(2,4,6-trimethylbenzoyl) phenylphosphine oxide, anhydrous sodium sulfate, zinc chloride, Sodium hydroxide and acryloyl chloride, were purchased from J&K Scientific Ltd.. The solvents used such as methylene chloride, triethylamine, 1,2-propanediol, diethyl ether and petroleum ether were purchased from Sinopharm Chemical Reagent Co., Ltd..

2.2. Measurements

FT-IR spectra of the synthesized polymers were measured on a Nicolet Nexus FT-IR spectrometer in the 4000~400 cm^{-1} region. The ^{1}H NMR spectra of the synthesized polymers were recorded in a $CDCl_3$ medium on a Bruker-400 spectrometer (400 MHz). UV-visible spectrometer (UV-3600 Shimadzu, Japan) was used to examine the transmittance of the UV-cured PPF/PPF-DA composite materials. The refractive indexes of the cured samples were detected using spectroscopic ellipsometer (PZ-2000 Jobin Yvon S.A.S, French). Thermogravimetric analyses (TGA) were carried out on a Perkin-Elmer Pyris-1 analyzer with a heating rate of 10 $^{o}C \cdot min^{-1}$ and a dry-nitrogen flow at 20 $mL \cdot min^{-1}$. Different scanning calorimeter measurements were performed on a Netzsch DSC 200 PC thermal analysis apparatus in a nitrogen atmosphere. The mechanical properties of the UV-cured samples were tested on a INSTRON 1195 mechanical testing system.

2.3. Syntheses

2.3.1. Synthesis of poly(propylene fumarate)

PPF was synthesized by a two-step reaction process described previously.[16] (**Scheme 1**) In the first step, diethyl fumarate (25.8 g, 150 mmol) and 1,2-propanediol (34.2 g, 450 mmol) were reacted in nitrogen atmosphere with a molar ratio of 1:3. Additionally, hydroquinone (0.03 g, 0.15 mmol) and zinc chloride (0.2 g, 1.5 mmol) were added the above reaction as a catalyst and cross-linking inhibitor, respectively. In this step, the reaction was performed in a heated vessel under mechanical stirring, with a gradual increase in temperature from 110 ^{o}C to 140 ^{o}C. Production harvested in this stage was the bis(hydroxypropyl) fumarate intermediate which stored in methylene chloride and the ethanol distillate was collected.

The second step of the synthesis reaction involved transesterification of the bis(hydroxypropyl) fumarate intermediate to PPF. In this step, the formed bis(hydroxypropyl) fumarate stored in methylene chloride firstly experienced a filtration and evaporation stage to remove the solvent, and then underwent a continuous heating for 7 h at a temperature of 130 ^{o}C and a low pressure of 5 mmHg to produce PPF. Purification of the PPF product occured through dissolution of the polymer in methylene chloride followed by several acid washes to remove the zinc chloride catalyst. PPF was purified through solution precipitation in chloroform and petroleum ether. Selected IR (KBr pellet, cm^{-1}): ν(-OH) 3540; ν(C-H) 2985; ν(C=O) 1731; ν(C=C) 1647; ν(-CH, -CH_2, -CH_3) 1456; ν(-C=CH-) 978. ^{1}H NMR(400 MHz, $CDCl_3$): δ 6.88(bs, 2H, -CH=CH-), 5.32(s, 1H, CH), 4.36~4.25(m, 2H, CH_2), 1.38~1.36(m, 3H, CH_3).

2.3.2. Synthesis of poly(propylene fumarate)-diacrylate

Scheme 1 shows the synthetic reactions of PPF-diacrylate. A typical procedure for synthesis of PPF-DA was given here. Bis(hydroxypropyl) fumarate was obtained from the reaction of diethyl fumarate with 1,2-propanediol as described above.

Fumaryl chloride (15.3 g, 100 mmol) was added dropwise to a solution of 1,2-propanediol (22.8 g, 300 mmol) in methylene chloride (40 mL) at 0 ^{o}C under nitrogen in the presence of anhydrous potassium carbonate (20.7 g, 150 mmol). After addition of fumaryl chloride, the reaction mixture was stirred overnight at room temperature and then water was added to dissolve the inorganic salt. The organic layer was separated and dried with anhydrous sodium sulfate. After filtration and evaporation of the solvent, the bis(hydroxypropyl) fumarate was obtained. Selected IR (KBr pellet, cm^{-1}): ν(-OH) 3433; ν(C-H) 2980; ν(C=O) 1726; ν(C=C) 1643; ν(-CH, -CH_2, -CH_3) 1455; ν(-C=CH-) 984.

To a solution of bis(hydroxypropyl) fumarate (11.6 g, 50 mmol) in dry methylene chloride (40 mL) at 0 ^{o}C was added triethylamine (15.2 g, 150 mmol). After stirring for 30 min, acryloyl chloride (9.5 g, 105 mmol) was added dropwise during approximately 2 h, causing formation of a white precipitate. The reaction mixture was stirred overnight at room temperature. The white precipitate was filtered off and the methylene chloride solvent was rotary evaporated. Diethyl ether (20 mL) was added to the residue and the ethyl acetate solution was washed with aq. NaOH (5%), water and brine. After drying over anhydrous sodium sulfate, filtration of the mixture and solvent evaporation, PPF-DA was obtained. Selected IR (KBr pellet, cm^{-1}): ν(C-H) 2984; ν(C=O) 1725; ν(-CH, -CH_2, -CH_3) 1451; ν(C-O-C) 1153; ν(-C=CH-) 975. ^{1}H NMR(400 MHz, $CDCl_3$): δ 6.87(bs, 2H, -CH=CH-), 6.43(dd, J=17.2Hz, 1H, -CH=CH_2), 6.17~6.09(m, 1H, -CH=CH_2), 5.89~5.86(m, 1H, -CH=CH_2), 5.33~5.27(m, 1H, CH), 4.36~4.20(m, 2H, CH_2), 1.36~1.33(m, 3H, CH_3).

2.4. Preparation of LED encapsulation material

Polymer networks were prepared by mixing PPF and PPF-DA in the appropriate amounts dictated by the double bond ratio (1:2, 1:1, 2:1) (**Scheme 1**). The double bond ratio was defined as the fraction of fumarate bonds within the PPF structure to the acrylate bonds of PPF-DA. PPF and PPF-DA were combined together by first dissolving

each component in methylene chloride. The two solutions were then added and stirred for 30 min. The mixture was rotary evaporated and vacuum dried to remove the solvent. Photo-crosslinking was accomplished with BAPO accelerated by UV irradiation. Initiator solution (0.1 g BAPO per 1 mL methylene chloride) was then added to the PPF/PPF-DA mixture. The paste was vigorously mixed and painted on the glass mould. The molds were placed in an OmniCure(SERIES2000) UV light box. Inside the box, samples were positioned roughly 10 cm below bulb that provided the majority of light at 365 nm and an intensity of approximately 300 $mw \cdot cm^{-2}$ within 5 minutes. Photographs of the prepared encapsulation material before and after UV-curable as shown in **Fig. 2**.

Scheme 1 Synthesis of PPF/PPF-DA polymer networks

Fig. 2 Photographs of the prepared LED encapsulation material before and after UV-curable.

2.5. Optical properties

UV-visible spectrometer (UV-3600 Shimadzu, Japan) was used to examine the transmittance of the LED packaging material. Both the bare PET for the control and the sample, which was coated on the PET film, were set on the instrument. The transmittance was determined in the visible range of 400-800 nm. The refractive index of the sample coated on a PET film was detected using spectroscopic ellipsometric (PZ-2000 Jobin Yvon S.A.S, French).

2.6. Temperature programmed combustion

The experiments were performed in a Perkin-Elmer Pyris-1 thermogravimetric analyzer with the sample mass loss percentage as functions of time or temperature recorded continuously under the temperature programmed combustion. During the experiments, the temperature increased from 25 to 1000 ^{o}C at a linear heating rate of 10 $^{o}C/min$. At the same time, the chamber blowing gas, N_2 (99.99% purity), was fixed at 20 $mL \cdot min^{-1}$. When data derived from TG curves were analyzed, they would be dealt with taking the original sample mass into consideration to eliminate the effect of mass different on the process. The detailed TG curves and educed data are shown in corresponding section which validates the stability of the experimental system. Differential scanning calorimeter data (DSC, Netzsch DSC 200 PC) were measured in a nitrogen atmosphere to study the thermal photo-crosslinked PPF/PPF-DA networks curing behavior of the mixed BAPO. All the specimens were first heated to 220 °C and maintained at 220 °C for 5 min to remove the influence of background, and then quenched to 30 °C, followed by heating from 30 °C to 220 °C with a heating rate of 5 °C/min.

2.7. Mechanics performance test

Two types of mechanical testing, tensile-shear strength and bonding strength, were conducted with cross-linked specimens at room temperature using an material testing system mechanical testing machine (INSTRON 1195) with five specimens tested for each sample group. Tensile-shear strength testing was carried out in accordance to the Adhesives-determination of tensile shear strength of rigid to rigid bonded assemblies (GB/T 7124-2008/ISO 4587: 2003). Bonding strength testing was performed in accordance to Adhesives-determination of tensile strength of butt joint (GB/T 6329-1996 eqv ISO 6922: 1987). For specimen preparation, the crosslinking mixture was placed into rectangle mold (length*width*thickness=10 mm*10 mm*1 mm). Samples were stretched at a crosshead speed of 1 mm/min until failure with the load versus deformation curve recorded throughout.

3. Results and discussions

3.1. Chemistry

A number of synthetic techniques for poly(propylene fumarate) have been reported.[22-24] More recently, the common method for synthesizing poly(propylene fumarate) follows a two-step procedure, beginning with diethyl fumarate and 1,2-propanediol, and involving bis(hydroxypropyl) fumarate as an intermediate (**Scheme 2**). This is the present method of PPF synthesis that is used in our research. The synthesis of PPF-DA and PPF were similar. These polymers were characterizated by IR spectra and ^{1}H NMR. The compounds were soluble in dichloromethane, acetone and trichloromethane.

Scheme 2 Synthesis of poly(propylene fumarate) (PPF) and PPF-diacrylate (PPF-DA)

Wave numbers of the selected vibration of IR spectra of the polymers are listed in **Fig. 3** of the experimental section. The IR spectra of the polymers were compared with the oligomer intermediate. Pertinent peaks of PPF-DA examined were carbonyl stretching at 1725 cm^{-1}, alkene C=C peak at 1643 cm^{-1}, methylene scissoring and methyl asymmetric bend in the 1451 cm^{-1} region, C-O stretch at 1153 cm^{-1} and C-H bend due to the double bond at 975 cm^{-1}. Further evidence for reaction at both ends came from the FTIR spectrum of PPF-DA, which showed no OH stretching band appeared in the region of 3500-3100 cm^{-1}. IR spectra were especially valuable for the characterization of the oligomer intermediate and PPF. The IR spectrum of oligomer intermediate showed the following characteristic bands: a broad OH stretch centered at 3433 cm^{-1}, ester carbonyl at 1726 cm^{-1}, and C=C stretch at 1643 cm^{-1}. After transesterication of the intermediate, a noticeable decrease of the OH band at 3433 cm^{-1} was observed because of the removal of end 1,2-propanediol. The change of IR spectra strongly supported the progress of transesterication. The spectra also corroborate previous characterizations of the PPF polymeric.

Fig. 3 FTIR spectra of PPF, PPF oligomer and PPF-DA are presented in 4000-400 cm^{-1} range.

^{1}H NMR spectra of the polymers were recorded in $CDCl_3$ taking using TMS as an internal standard. ^{1}H NMR spectra data for the polymers are given in experimental, respectively. It is known that symmetric H atoms in the compounds have the same chemical shift because of the same chemical environment of the atoms. Chemical Shift values of the polymers are in reasonable agreement with literature data for the similar compounds.[17] In **Fig. 4**, four multiplets were observed. Seven multiplets were observed in **Fig. 5**. The signal at 6.88 ppm and 6.87 ppm were assigned to the olefinic protons while the 1.38 ppm-1.33 ppm peak was attributed to the methyl protons. The other two signals at 5.33 ppm-5.27 ppm and 4.36 ppm-4.20 ppm belonged, respectively, to the methine and methylene protons of the propyl diol. Difference in the chemical shift might be attributed to the formation of intermolecular interactions with solvent.

Fig. 4 ^{1}H NMR spectrum of PPF.

Fig. 5 ^{1}H NMR spectrum of PPF-diacrylate.

3.2. Optical properties

The transmittance of composite material was measured by UV-visible spectrometer. In this study, the PPF/PPF-DA polymers were coated on a PET film. Hence, the bare PET film was used as the reference. **Fig. 6** shows the relationships between transmittance and wavelength for the prepared encapsulation material before and after thermal degradation aging. Thermal aging studies were conducted in a electric constant temperature drying oven. Test temperature was 150 ^{o}C and aging time was one week. In the visible light region, the cured PPF/PPF-DA

encapsulation material is glassy with a high transparency of 98.75%. The PPF/PPF-DA polymer networks material has high light transmittance even after thermal degradation, in order to be used in optical films. The network structure was therefore influenced by the amount of acrylates present in the reagent formulation, which increases with decreasing double bond ratio. PPF/PPF-DA networks of double bond ratio 1 shows strong degradataion after thermal aging, while the other two show relatively minimal effect. Increasing the PPF content within the reagent formulation results in a greater viscosity, which can limit the double bond conversion by diffusion limitations.[18] This prepared encapsulation material exhibits super stability towards heat thanks to the cross-linking of the polymer into a covalent polymer network, enabling long life performance of high brightness LEDs with little intensity degradation. The refractive index of a LED encapsulant is the main factor to develop high luminescence efficiency in a white LED through enhancement of the light extraction efficiency. This encapsulation material has a higher refractive index (n=1.537-1.541) in the visible range (**Fig. 7**). Generally, the cross-linked polymer containing a higher refractive index functional group in comparison with its monomer. The refractive index is dependent on the wavelength, with the real part of the refractive index decreasing with increasing wavelength. In this regard, the crosslinking reaction caused the increase in refractive index of PPF/PPF-DA, particularly in the wavelength range of 400-800 nm.

Fig. 6 Relative transmittance of the PPF/PPF-DA polymer networks before and after thermal aging(one week).

Fig. 7 The refractive index of PPF/PPF-DA polymer networks in the visible range.

3.3. Thermal behavior analysis

Usually, a LED chip always generated heat and thus degrade the performance of individual components in the LED, so the thermal stability of LED encapsulant is worth being investigated. The thermal properties of the encapsulation material under nitrogen were studied by differential scanning calorimeter (DSC) and thermal gravimetric analysis (TGA). In the present study, thermogravimetric analysis was carried out to examine the thermal stability of the polymers. The different proportions of sample was heated up to 1000 ^{o}C in N_2 at a heating rate of 10 ^{o}C·min^{-1}. The stages of decomposition, temperature range as well as the weight loss percentages of the polymers are shown in **Fig. 8**. The experimental weight loss values are in good agreement with the calculated values. The curves of encapsulation material and values of glass transition temperatures from DSC are shown in **Fig. 9** (heating rate: 5 ^{o}C·min^{-1}).

Fig. 8 Thermal analysis curves of the PPF/PPF-DA polymer networks with a double bond ratio of 0.5, 1, and 2.

Fig. 9 DSC spectra of the already UV-crosslinked PPF/PPF-DA networks with double bond ratio 0.5, 1, and 2.

Observed from **Fig. 8**, PPF/PPF-DA polymer networks with a double bond ratio of 0.5 keeps thermal-stability up to 287.98 ^{o}C without any weight loss, which means the compound could retain structural integrity above this temperature. However, the composite material undergoes one major stage of weight loss between 287.98 ^{o}C and 483.28 ^{o}C, and the endothermic peak is in the temperature of 368.56 ^{o}C. The total weight loss at this stage closes to 81.55%. In **Fig. 8**, one obvious weight loss of PPF/PPF-DA networks with a double bond ratio of 1 can be clearly identified, which starts from 285.26 ^{o}C and ends at 473.47 ^{o}C with a sum loss of 79.55%. The endothermic peak appeared at the temperature of 367.36 ^{o}C. Additionally, a mass loss stage is observed on the TG curves of networks of with a double bond ratio of 2, shown in **Fig. 8**, and the stage started from 271.60 ^{o}C and ended at 475.39 ^{o}C with a sum loss of 80.09%, and the endothermic peak is in the temperature of 365.29 ^{o}C. In summary, the double bond

ratio play a considerable role in the thermal-stability of the PPF/PPF-DA crosslinking networks. The novel UV-cured encapsulation material gets most excellent thermal-stability with a double bond ratio of 0.5.

Fig. 9 shows the results obtained using DSC, which indicates the curing behavior of the already UV-crosslinked PPF/PPF-DA networks with double bond ratios of 0.5, 1, and 2. The spectra shows an exothermic of the polymer by crosslinking. The onset curing temperature decreases from 166.61 ^{o}C to 139.28 ^{o}C by modifying the structure and double bond ratios of the polymer. The glass transition temperature (Tg) can be located from the steep slope due to the phase change. The Tgs of the three different double bond ratios material were 177.92 ^{o}C, 154.36 ^{o}C, and 161.44 ^{o}C, respectively. Also, the enthalpy change (ΔH) of the encapsulation material are -14.69 J/g, -3.10 J/g, -6.26 J/g, with double bond ratios of 0.5, 1, and 2, respectively. The reaction continues to a temperature of 194.7 ^{o}C. Due to the steric consequences of different double bond ratios in the PPF/PPF-DA polymer networks, the cross-linking did not fully occur in the encapsulation material. The rate of the curing (with double bond ratios of 0.5) were slower than that of the other two. Un-crosslinked propylene fumarate groups can be the source of the discoloration of the encapsulation material during thermal aging. Thus, we need a very high temperature, strong UV light and long curing time for the fabrication of networks with the BAPO initiator in an efficient dose range.

3.4. Mechanical properties

PPF/PPF-DA composite materials has been shown to be a versatile material in which its mechanical properties can be altered by the initiator system or the crosslinking ratio.[17] The tensile-shear strength and bonding strength of the UV-crosslinked PPF/PPF-DA polymer networks with double bond ratios of 0.5, 1, and 2, respectively, are shown in **Fig. 10**. For the PPF/PPF-DA photo-crosslinked with BAPO and UV light, the bonding strength was in the range of 1.09±0.04 MPa to 2.39±0.04 MPa. The tensile-shear strength ranged from 0.38±0.02 MPa to 0.79±0.03 MPa. These results demonstrate that the mechanical properties of PPF/PPF-DA polymeric networks can be tailored by varying the PPF/PPF-DA double bond ratio. In comparison with other cross-linked PPF composites, the PPF/PPF-DA polymer networks tested in this study showed improved mechanical properties.[13, 25]

The bonding strength of the UV-cured PPF/PPF-DA material with a double bond ratio of 0.5 (2.35±0.04 MPa) was found to be significantly stronger than the networks with double bond ratio of 1 (1.14±0.04 MPa) and 2 (1.43± 0.03 MPa). Their tensile-shear strength testing results showed no significant difference was identified between the strength values with double bond ratio of 1 (0.45±0.02 MPa) and 2 (0.40±0.02 MPa) but a more than 70% increase appeared in the strength values of PPF/PPF-DA polymer networks of double bond ratio 0.5 (0.73±0.03 MPa) compared to 1 and 2. It indicates that the mechanical properties of the UV-crosslinked networks significantly decrease with increasing their double bond ratio. For the BAPO initiator in an efficient dose range, both the tensile-shear and bonding strengths of PPF/PPF-DA polymer networks depended on the numbers of acrylate bonds participating in the crosslinking reaction. These results demonstrate that the double bond ratio is a critical parameter for adjusting the mechanical properties of the PPF/PPF-DA polymer networks. From a viewpoint of mechanical property, this kind of PPF/PPF-DA network is suitable for the application of LED encapsulant.[3,26-27]

Fig. 10 The tensile-shear strength and bonding strength of the PPF/PPF-DA polymer networks of double bond ratio 0.5, 1, and 2 (Error bars represent mean±SD for n=5).

4. Conclusions

In this paper a novel poly(propylene fumarate)-based LED encapsulation material was proposed. PPF and PPF-DA had been successfully prepared from readily available starting compounds with convenient procedure. The degree of completion of the curing reaction was increased with increasing ultraviolet illumination time. There was an increase in the tensile-shear and bonding strength when the double bond ratio of PPF/PPF-DA decreased resulting

from more acrylate bonds participating in the crosslinking reaction. The fabricated encapsulation material showed excellent optical transparency with high refractive index. Also, the mechanical properties and excellent thermal stability were examined to confirm its feasibility for use as an encapsulant for LEDs. These parameters are strikingly effective properties for high performance LED encapsulants. In a word, this kind of PPF/PPF-DA polymer network is suitable for the application of LED encapsulant. Our efforts are ongoing in this field and further work will be reported subsequently in the future.

Conflict of interest

The author(s) confirms that this article content has no conflicts of interest.

Acknowledgments

This work was supported by the National Natural Science Foundation of China (No.51273159) and Fundamental Research Funds for the Central University.

References

1 Y. S. Su, *Int. J. Photoenergy*., 2014, **2014**, 735983.

2 N. Gao, W. Liu, S. Ma, C. Tang and Z. J. Yan, *J. Polym. Res*., 2012, **19**, 9923-9932.

3 M. Zhao, Y. K. Feng, Y. Li, G. Li, Y. L. Wang, Y. Han, X. J. Sun and X. H. Tan, *J. Macromol. Sci. A*., 2014, **51**, 653-658.

4 J. P. You, Y. C. Shih, Y. H. Lin, B. Yan and F. G. Shi, *ECTC*., 2012, 2117-2120.

5 M. A. Tehfe, F. Dumur, P. Xiao, J. Zhang, B. Graff, M. S. Fabrice, D. Gigmes, J. P. Fouassier and J. Lalevée. *Polymer*., 2014, **55**, 2285-2293.

6 J. C. Huang, Y. P. Chu, M. Wei and R. D. Deanin, *Adv. Polym. Technol*., 2004, **23**, 298-306.

7 A. W. Norris, M. Bahadur and M. Yoshitake, *Proc. of. SPIE*., 2005, **5941**, 594115-7.

8 N. Chikhi, S. Fellahi and M. Bakar, *Eur. Polym. J*., 2002, **38**, 251-264.

9 W. Huang, Y. Zhang, Y. Z. Yu and Y. X. Yuan, *J. Appl. Polym. Sci*., 2007, **104**, 3954-3959.

10 M. J. Yaszemski, R. G. Payne, W. C. Hayes, R. Langer and A. G. Mikos, *Biomaterials*, 1996, **17**, 175-185.

11 G. B. Kharas, M. Kamenetsky, J. Simantirakis, K. C. Beinlich, A. T. Rizzo, G. A. Caywood and K. Watson, *J. Appl. Polymer. Sci*., 1997, **66**, 1123-1137.

12 T. N. Gerhart, A. A. Renshaw, R. L. Miller, R. J. Noecher and W. C. Hayes, *J. Biomed. Mater. Res*., 1999, **44**, 314-322.

13 A. J. Domb, N. Manor and O. Elmalak, *Biomaterials*, 1996, **17**, 411-417.

14 J. D. Gresser, S. H. Hsu, H. Nagaoka, C. M. Lyons, D. P. Nieratko, D. L. Wise, G. A. Barabino and D. J. Trantolo, *J. Biomed. Mater. Res*., 1995, **29**, 1241-1247.

15 M. D. Timmer, C. G. Ambrose and A. G. Mikos, *Biomaterials*, 2003, **24**, 571-577.

16 F. K. Kasper, K. Tanahashi, J. P. Fisher, A. G. Mikos, *Nat. Protoc*., 2009, **4**, 518-525.

17 S. He, M. D. Timmer, M. J. Yaszemski, A. W. Yasko, P. S. Engel and A. G. Mikos, *Polymer*, 2001, **42**, 1251-1260.

18 M. D. Timmer, S. Jo, C. Wang, C. G. Ambrose and A. G. Mikos, *Macromolecules*, 2002, **35**, 4373-9.

19 B. D. Porter, J. B. Oldham, S. L. He, M. E. Zobitz, R. G. Payne, K. N. An, B. L. Currier, A. G. Mikos and M. J. Yaszemski, *J. Biomech. Eng*., 2000, **122**, 286-288.

20 M. D. Timmer, R. A. Horch, C. G. Ambrose and A. G. Mikos, *J. Biomater. Sci. Polym. Ed*., 2003, **14**, 369-382.

21 T. Otsu, A. Matsumoto, K. Shiraishi, N. Amaya and Y. Koinume, *J. Polym. Sci., Part A: Polym. Chem*, 1992,

30, 1559-1565.

22 A. K. Shung, M. D. Timmer, S. Jo, P. S. Engel and A. G. Mikos, *J. Biomater. Sci. Polym. Ed*., 2002, **13**, 95-108.

23 S. J. Peter, M. J. Yaszemski, L. J. Suggs, R. G. Payne, R. Langer, W. C. Hayes, M. R. Unroe, L. B. Alemany, P. S. Engel and A. G. Mikos, *J. Biomater. Sci. Polym. Ed*., 1997, **8**, 893-904.

24 S. J. Peter, L. J. Suggs, M. J. Yaszemski, P. S. Engel and A. G. Mikos, *J. Biomater. Sci. Polym. Ed*., 1999, **10**, 363-373.

25 U. Kandalam, A. J. Bouvier, S. B. Casas, R. L. Smith, A. M. Gallego, J. K. Rothrock, J. Y. Thompson, C. -Y. C. Huang, E. J. Stelnicki, *Int. J. Oral Maxillofac. Surg*., 2013, **42**, 1054-1059.

26 J. Y. Bae, Y. H. Kim, H. Y. Kim, Y. W. Lim and B. S. Bae, *RSC Adv*., 2013, **3**, 8871-8877.

27 J. C. Huang, Y. P. Chu, M. Wei and R. D. Deanin, *Adv. Polym. Tech*., 2004, **23**, 298-306.

Scheme 1 Synthesis of PPF/PPF-DA polymer networks

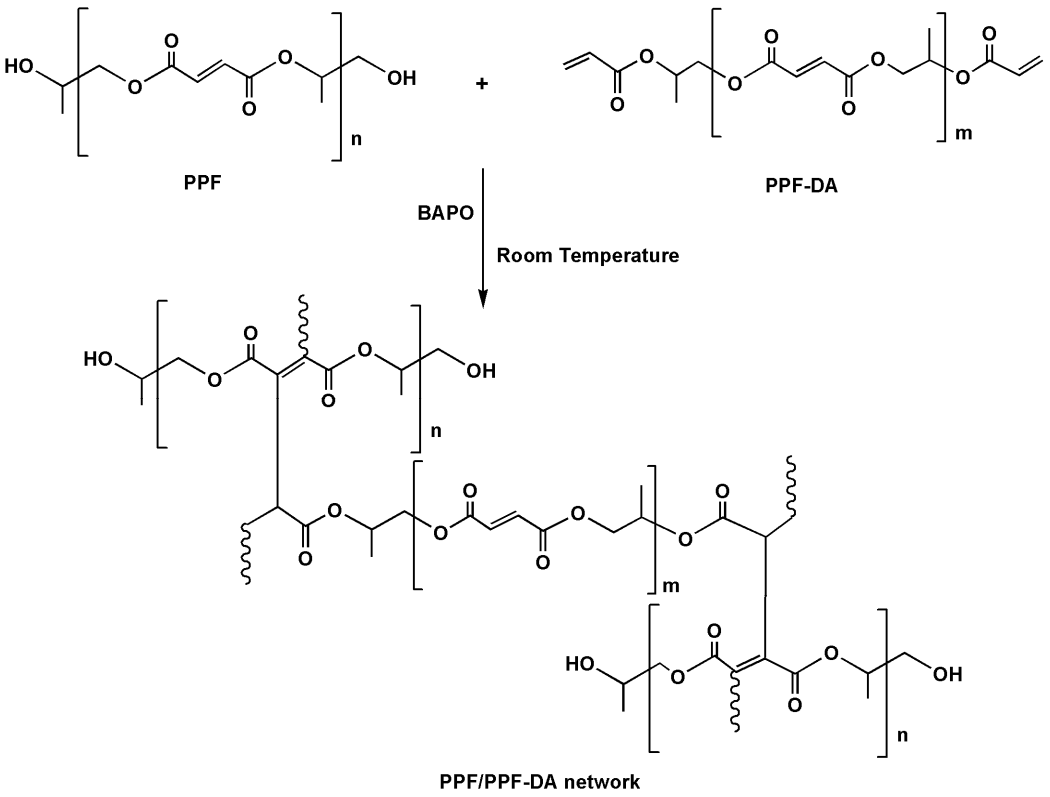

Scheme 2 Syntheses of poly(propylene fumarate) and PPF-diacrylate

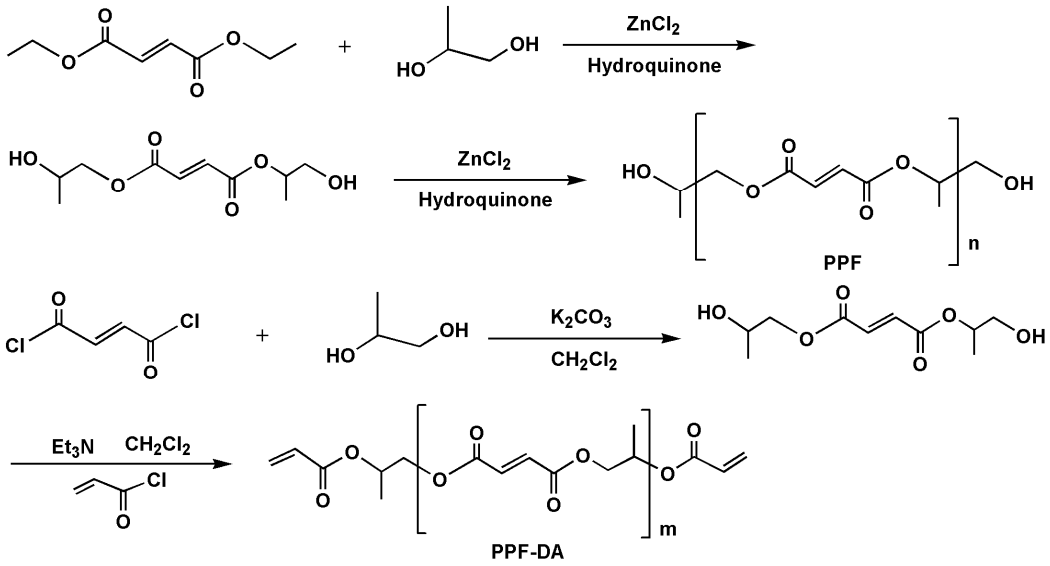

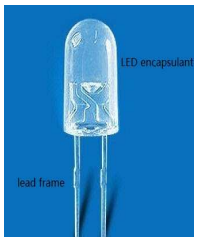

Fig. 1 Photograph of the Light emitting diode (LED).

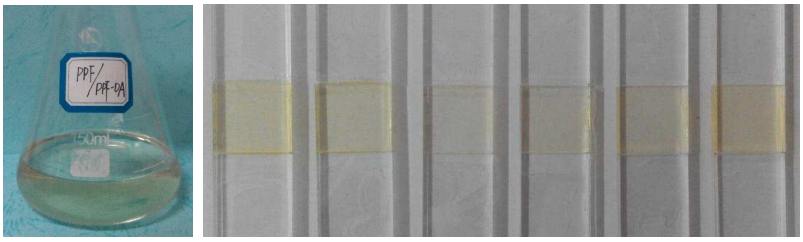

Fig. 2 Photographs of the prepared LED encapsulation material before and after UV-curable.

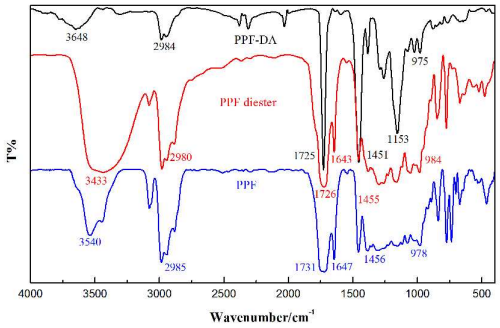

Fig. 3 FTIR spectra of PPF, PPF oligomer and PPF-DA are presented in 4000-400 cm^{-1} range.

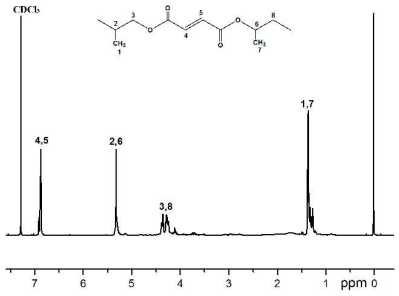

Fig. 4 ^{1}H NMR spectrum of PPF.

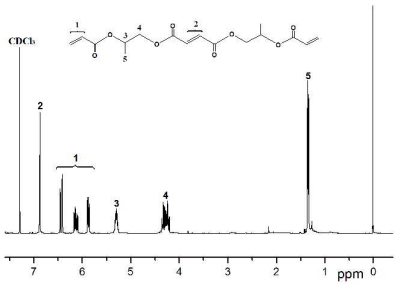

Fig. 5 ^{1}H NMR spectrum of PPF-diacrylate.

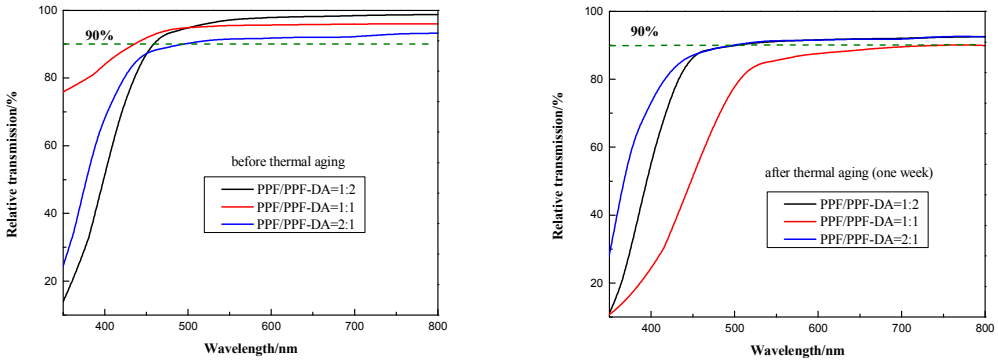

Fig. 6 Relative transmittance of the PPF/PPF-DA polymer networks before and after thermal aging(one week).

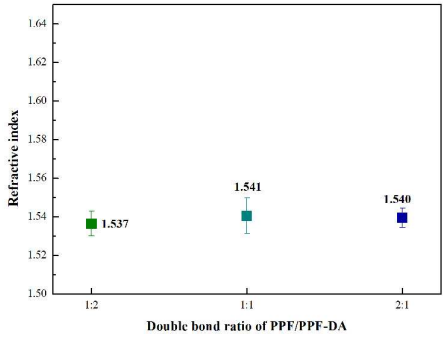

Fig. 7 The refractive index of PPF/PPF-DA polymer networks in the visible range.

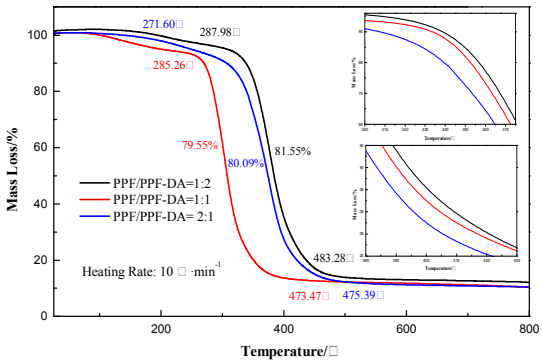

Fig. 8 Thermal analysis curves of the PPF/PPF-DA polymer networks with a double bond ratio of 0.5, 1, and 2.

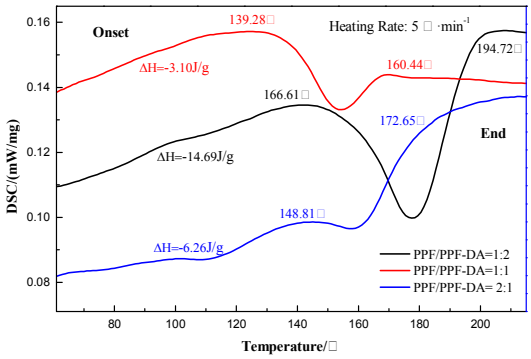

Fig. 9 DSC spectra of the already UV-crosslinked PPF/PPF-DA networks with double bond ratio 0.5, 1, and 2.

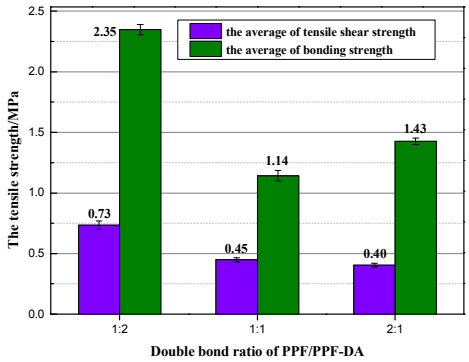

Fig. 10 The tensile-shear strength and bonding strength of the PPF/PPF-DA polymer networks of double bond ratio 0.5, 1, and 2 (Error bars represent mean±SD for n=5).